

Time evolution of the second magnetization peak in $\text{Bi}_2\text{Sr}_2\text{CaCu}_2\text{O}_{8+\delta}$

B. Kalisky and A. Shaulov

Institute of Superconductivity, Department of Physics, Bar-Ilan University, Ramat-Gan 52900, Israel

T. Tamegai

Department of Applied Physics, The University of Tokyo, Hongo, Bunkyo-ku, Tokyo 113-8656, Japan

Y. Yeshurun

Institute of Superconductivity, Department of Physics, Bar-Ilan University, Ramat-Gan 52900, Israel

(Presented on 15 November 2002)

Local magnetization curves at different times, extracted from high-temporal resolution magneto-optical measurements in $\text{Bi}_2\text{Sr}_2\text{CaCu}_2\text{O}_{8+\delta}$, demonstrate the absence of the second magnetization peak at short times, its appearance at longer times, and the movement of its onset toward higher-induction fields approaching the thermodynamic vortex order–disorder transition field. We relate this phenomena to metastable disordered states induced by edge contamination for inductions in the vicinity of the order–disorder vortex phase transition. We show that the time evolution of the second magnetization peak is governed by the relaxation times of the metastable disordered vortex states. © 2003 American Institute of Physics. [DOI: 10.1063/1.1556287]

It is now well established that the sharp onset of the second magnetization peak (fishtail) in $\text{Bi}_2\text{Sr}_2\text{CaCu}_2\text{O}_{8+\delta}$ signifies a vortex phase transition from a weakly pinned vortex lattice to a strongly pinned disordered vortex phase.¹ However, several phenomena related to the fishtail still remain to be reconciled with the vortex phase transition scenario; e.g., smearing of the fishtail as the temperature is lowered until below ~ 17 K it disappears altogether,^{2,3} reappearance of the fishtail in longer time scales, and a shift of its onset with time towards higher fields.³

In this article, we employ a high-temporal resolution magneto-optical system to follow the time evolution of the fishtail. Our measurements reveal that the fishtail is shaped by metastable disordered vortex states, injected into the sample through inhomogeneous surface barriers.⁴ At low temperatures, the lifetime of these metastable states is long enough to obscure the sharp magnetic signature of the thermodynamic order–disorder phase transition.⁵ As the induced disordered metastable states decay, the fishtail appears. We conclude that the relaxation process of the induced disordered metastable states governs the time evolution of the fishtail.

Measurements were performed on a $1.55 \times 1.25 \times 0.05$ mm³ $\text{Bi}_2\text{Sr}_2\text{CaCu}_2\text{O}_{8+\delta}$ single crystal ($T_c \sim 92$ K). The external magnetic field H was raised abruptly to a target value between 140 and 840 G with rise-time < 50 ms. Immediately after reaching the target field, magneto-optical (MO) snapshots of the induction distribution across the sample surface were recorded at time intervals of 40 ms for 4 s, and 200 ms for an additional 26 s, using iron-garnet MO indicator and a high-speed charge-coupled device camera.

Figure 1 shows the time evolution of the induction profiles after abruptly increasing the external field H to 340, 500, and 600 G. (The profiles at $t = 0.04, 0.12, 0.16, 0.28, 0.4, 0.8, 1.6, 3.72,$ and 29 s are bolded, to match the time

evolution curves shown in Fig. 2, as described below). Figure 1(a) presents the induction distribution across the entire sample width, whereas Figs. 1(b)–1(d) focus on the interesting part of the profiles, near the sample edge. The profiles of Fig. 1 are characterized by a sharp change in the slope (a “break”) at a time-dependent location x_f . The breaks separate between a high-persistent current region near the sample edges and a low-persistent current region near the sample center. The time dependence of x_f varies with H . In Fig. 1(b), the break moves towards the sample edge until it disappears, leaving the entire sample in the low-persistent current state. A similar, but slower motion of x_f is observed in Fig. 1(c). In Fig. 1(d), the break moves towards the center of the sample

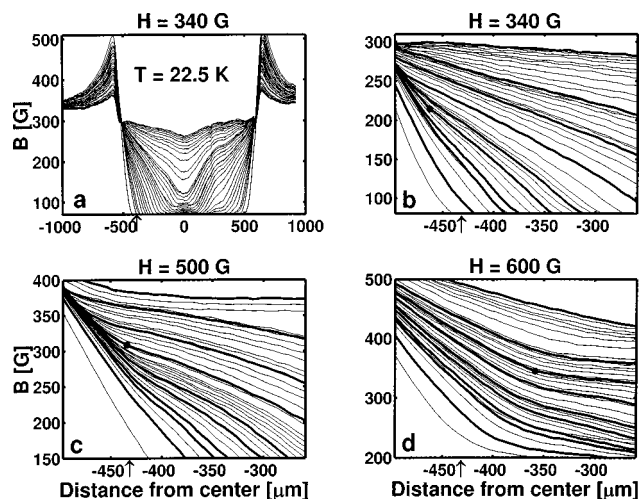


FIG. 1. Time evolution of the magnetic induction profiles at $T = 22.5$ K, after a step increase of the external magnetic field to 340 G (a and b); 500 G (c); and 600 G (d) during 30 s after field application. Bolded profiles match times indicated in Fig. 2. Dots in (b)–(d) mark typical breaks in the profiles. Arrows point to the location $x_0 = -437$ μm .

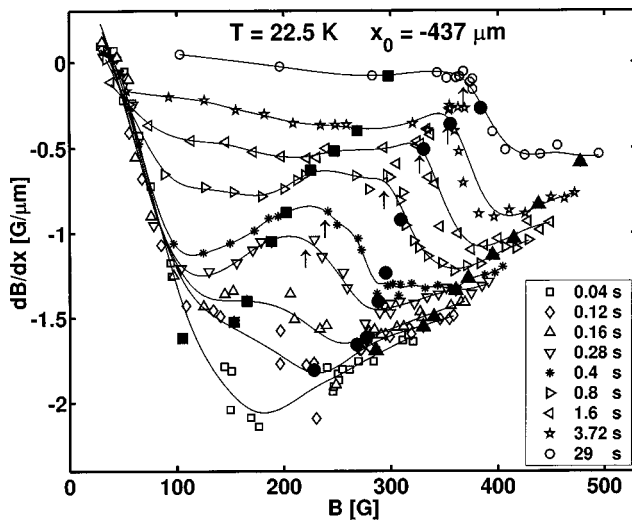


FIG. 2. j vs local B at $x_0 = -437 \mu\text{m}$ for the indicated times. Bold symbols describe the time dependence of j for the three external fields presented in Fig. 1 (squares, circles, and triangles for 340, 500, and 600 G, respectively). Arrows indicate fishtail onset.

and eventually the entire sample is in a high persistent current state.

Similar results were previously reported by Giller *et al.*⁶ and were interpreted in the following way: By abruptly increasing the field, vortices injected through inhomogeneous surface barriers generate a transient disordered state. These transient states anneal at a characteristic time $\tau(B)$.⁵ The break in the profiles separates between the transient disordered state (high- j) near the edge and the quasiordered phase (low- j) near the center.

From the time evolution of the profiles at various H , we extract the time evolution of the local $j \sim dB/dx$ versus B curves. Typical results are presented in Fig. 2 for location $x_0 = -437 \mu\text{m}$ measured from the sample center (marked by an arrow in Fig. 1). The solid lines in Fig. 2 connect all points measured at the same indicated time, for the various external fields. The times chosen to be presented in Fig. 2 match the bolded profiles in Fig. 1. Bold symbols in Fig. 2 describe the time dependence of j for the three external fields presented in Fig. 1 (squares, circles, and triangles for 340, 500, and 600 G, respectively).

The striking features exhibited in Fig. 2 are the absence of the fishtail at short times, its appearance at longer times, and the shift of its onset to higher inductions with time (from 200 at 0.28 s to 365 G at 29 s). Similar phenomena have previously been observed in various local and global measurements.^{2,3,7} Our experiments, however, are unique in enabling us to trace the dynamics of the fishtail (Fig. 2) to the dynamics of the profiles (Fig. 1). By comparing Figs. 1 and 2, we are able to propose an explanation for these features, as explained below.

We first characterize the vortex state at an arbitrary location x_0 as a function of its position relative to the break in the profile. If x_0 is between the break and the edge, then the vortex state at x_0 is a disordered state. On the other hand, if x_0 is between the break and the center, the vortex state at x_0 is a quasiordered state. Profiles without a break that precede

profiles with a break, signify a transient disordered state in the entire sample. Similar profiles, observed after the disappearance of the break, signify a quasiordered (disordered) phase at the entire sample, if the break disappears at the edge (center) of the sample. From the above notes, the following explanation for Fig. 2 emerges.

Figure 2 describes j versus B at $x_0 = -437 \mu\text{m}$. At short times, x_0 is located in a transient disordered region for all measured H . This is evident, for example, in Figs. 1(b)–1(d) where initially x_0 is between the break and the edge [Fig. 1(d)] or the break has not yet appeared [Figs. 1(b) and 1(c)]. The fact that transient states persist for all fields, results in the absence of the fishtail fingerprint in Fig. 2, namely, there is no jump from low- to high- j at short time.

As time progresses, the transient states anneal. As the annealing process is faster at low inductions, i.e., τ becomes shorter than our time window, the vortex state at x_0 is now ordered at these low inductions, see Fig. 1(b), for example. (At the second bolded profile, x_0 is already to the right of the break, i.e., in the ordered phase regime). At high fields, however, the state at x_0 is still disordered—see, for example, Fig. 1(c) (where at the second bolded profile, x_0 is still to the left of the break)—because τ is longer than the measurement time window. As a result, a fishtail, namely, a jump from low- to high- j can now be observed in the $j(B)$ curves of Fig. 2. At further longer times, the vortex state at x_0 anneals even for higher inductions, and therefore, the fishtail onset appears at higher inductions.

To explain the width of the transition from the low- j to the high- j phase in Fig. 2, we note that in data analysis we average over several neighboring pixels, and hence, x_0 has a width Δx . We refer to $x_0 \pm \Delta x$ as the “probed width.” The width of the transition reflects the induction range for which quasiordered and transient disordered states coexist in the probed width.

To conclude, transient disordered states obscure the thermodynamic order–disorder vortex phase transition at low temperatures, where the lifetime spectrum of transient states is wide⁵ and larger than the experimental time window even at low inductions. Our results are consistent with previous reports on the time evolution of the fishtail.^{2,3,7} Our results are unique, however, in enabling direct comparison between the dynamics of $j(B)$ and the dynamics of the profiles after an abrupt change in the external magnetic field. This allows for a direct observation of the field and time regimes of the coexistence of the quasiordered and transient disordered states, pointing to the significance of long-living transient disordered states in shaping the fishtail.

This manuscript is a part of B.K.’s Ph.D. thesis. A.S. acknowledges support from the Israel Science Foundation (ISF). This research is supported by The ISF-Center of Excellence Program, and by the Heinrich Hertz Minerva Center for High Temperature Superconductors.

¹B. Khaykovich, E. Zeldov, D. Majer, T. W. Li, P. H. Kes, and M. Konczykowski, *Phys. Rev. Lett.* **76**, 2555 (1996).

²Y. Yeshurun, N. Bontemps, L. Burlachkov, and A. Kapitulnik, *Phys. Rev. B* **49**, R1548 (1994).

³M. Konczykowski, C. J. van der Beek, S. Colson, M. V. Indenbom, P. H. Kes, Y. Paltiel, and E. Zeldov, *Physica C* **341**, 1317 (2000).

⁴Y. Paltiel *et al.*, *Nature (London)* **403**, 398 (2000).

⁵B. Kalisky, A. Shaulov, and Y. Yeshurun (submitted to LT23 conference).

⁶D. Giller, A. Shaulov, T. Tamegai, and Y. Yeshurun, *Phys. Rev. Lett.* **84**, 3698 (2000).

⁷H. Kupfer, A. Will, R. Meier-Hirmer, T. Wolf, and A. A. Zhukov, *Phys. Rev. B* **63**, 214 521 (2001).